

Iminochromene Inhibitors of Dynamins I and II GTPase Activity and Endocytosis

Timothy A. Hill,[†] Anna Mariana,[‡] Christopher P. Gordon,[†] Luke R. Odell,^{†,§} Mark J. Robertson,[†] Andrew B. McGeachie,[‡] Ngoc Chau,[‡] James A. Daniel,[‡] Nick N. Gorgani,[‡] Phillip J. Robinson,[‡] and Adam McCluskey^{*,†}

[†]Chemistry, School of Environmental and Life Sciences, The University of Newcastle, Callaghan, NSW 2308, Australia, and [‡]Cell Signaling Unit, Children's Medical Research Institute, The University of Sydney, Locked Bag 23, Wentworthville, Sydney, NSW 2145, Australia.

[§]Current address: Organic Pharmaceutical Chemistry, Department of Medicinal Chemistry, Uppsala Biomedical Centre, Uppsala University, Box 574, SE-751 23 Uppsala, Sweden.

Received January 28, 2010

Herein we report the synthesis of discrete iminochromene (“iminodyn”) libraries (**14–38**) as potential inhibitors of dynamin GTPase. Thirteen iminodys were active (IC₅₀ values of 260 nM to 100 μM), with *N,N*-(ethane-1,2-diyl)bis(7,8-dihydroxy-2-iminochromene-3-carboxamide) (**17**), *N,N*-(ethane-1,2-diyl)-bis(7,8-dihydroxy-2-iminochromene-3-carboxamide) (**22**), and *N,N*-(ethane-1,2-diyl)bis(7,8-dihydroxy-2-iminochromene-3-carboxamide) (**23**) (IC₅₀ values of 330 ± 70, 450 ± 50, and 260 ± 80 nM, respectively) being the most potent. Five of the most potent iminodys all inhibited dynamins I and II approximately equally. Iminodyn-**22** displayed uncompetitive inhibition with respect to GTP. Selected iminodys were evaluated for their ability to block receptor mediated endocytosis (RME, mediated by dynamin II) and synaptic vesicle endocytosis (SVE, mediated by dynamin I), with **17** showing no activity while **22** returned RME and SVE IC₅₀ values of 10.7 ± 4.5 and 99.5 ± 1.7 μM, respectively. The iminodys reported herein represent a new chemical class of the first nanomolar potent dynamin inhibitors that are also effective endocytosis inhibitors.

Introduction

Dynamin is a multifunctional enzyme involved in the endocytosis of clathrin-coated vesicles and caveolae, phagocytosis, podosome formation, some forms of actin rearrangement, centrosomal cohesion, and cytokinesis.^{1–3} Its GTPase activity is integrally involved in these processes. There are three dynamin genes, with dynamin I in neurons, II being ubiquitously expressed, and III in neurons and testes.^{5,7} The primary role of dynamins I and II appears to be in the mediation of two main forms of endocytosis. One is receptor-mediated endocytosis (RME⁶) mediated by dynamin II which is initiated upon ligand binding to cell surface receptors and occurs via clathrin-coated pits in most cells.⁴ The second is the rapid synaptic vesicle endocytosis (SVE) likely mediated by dynamin I that follows vesicle exocytosis in nerve terminals. SVE serves to retrieve empty synaptic vesicles for later

refilling.^{4,5} SVE and RME perform distinct functional roles although they share much of the same underlying protein machinery of a common process collectively called clathrin-mediated endocytosis (CME).

Dynamin was the first member of a small family of dynamin-like GTP-binding proteins that share similar GTPase domains. This domain is crucial for vesicle fission, and consequently represents an important step in the endocytic pathway.^{4,6} All dynamins have four main functional domains – GTPase;^{4,8} pleckstrin homology (PH);⁵ proline/arginine-rich domain (PRD);^{5,8} and GTPase effector domain (GED),⁹ all of which are potential drug targets.

Recent evidence has emerged that dynamin II plays a key role in the development of human diseases;¹⁰ Charcot-Marie-Tooth disease (CMT)¹¹ and in autosomal dominant centronuclear myopathy (CNM).¹² Alzheimer's disease, Huntington's disease, Stiff-person syndrome, Lewy body dementias, and Niemann-Pick type C disease are illustrative of human pathological conditions within which defects in endocytosis have been implicated.^{7,13–15} Endocytic pathways are also utilized by viruses, toxins and symbiotic microorganisms to gain entry into cells.¹⁶ Inhibition of the GTPase activity of dynamin may be a useful strategy to prevent infection by such pathogens.¹⁷

Multiple nonspecific endocytosis inhibitors and processes exist: cationic amphiphilic drugs, e.g., chlorpromazine,¹⁸ concanavalin A,¹⁹ phenylarsine oxide,¹⁹ dansylcadaverine;²⁰ intracellular potassium depletion;²¹ intracellular acidification;²² and decreasing medium temperature.¹⁸ Over the past few years our group reported on the first classes of endocytosis inhibitors that mediate their effects via dynamin

*To whom correspondence should be addressed. Phone: +61-2-4921-6486. Fax: +61-2-4921-5472. E-mail: Adam.McCluskey@newcastle.edu.au.

^a Abbreviations: RME, receptor mediated endocytosis; SVE, synaptic vesicle endocytosis; CME, clathrin-mediated endocytosis; GED, GTPase effector domain; PRD, proline rich domain; PH, pleckstrin homology; SH3, Src homology 3; CMT, Charcot–Marie–Tooth disease; CNM, centronuclear myopathy; MiTMAB, myristoyltrimethylammonium bromide; OcTMAB, octyltrimethylammonium bromide; Bis-T, bis-tyrphostin; RTIL, room temperature ionic liquid; SAR, structure–activity relationship; EGFR, epidermal growth factor receptor; Tf-TxR, Texas Red-Tf; U2OS, human bone osteosarcoma epithelial cells; PS, phosphatidylserine; PMSF, phenylmethylsulfonyl fluoride; PFA, paraformaldehyde; FCS, fetal calf serum; DMEM, Dulbecco's Modified Eagle's Medium; DMSO, dimethyl sulfoxide; IXM, Image-Xpress Micro; HEPES, 4-(2-hydroxyethyl)-1-piperazineethanesulfonic acid; FM 4-64, *N*-(3-triethylammoniumpropyl)-4-(4-diethylaminophenyl)hexatrienylpyridinium dibromide.

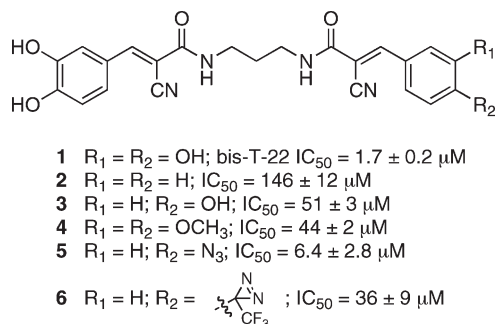


Figure 1. Chemical structures of selected Bis-T-22 analogues (**1–6**) and their IC_{50} values for inhibition of the GTPase activity of dynamin I (data are from ref 27).

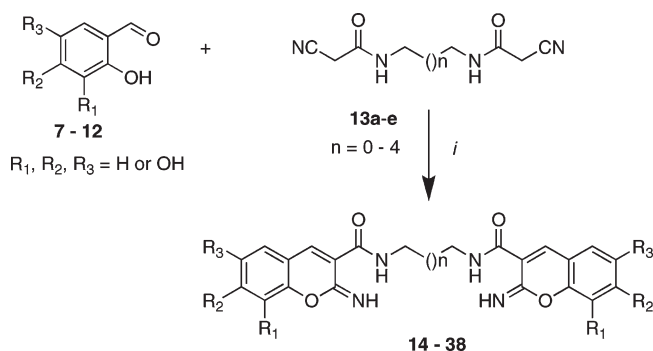
GTPase inhibition; the long chain amines and ammonium salts exemplified by myristoyltrimethylammonium bromide (MiTMAB),^{23,24} room temperature ionic liquids (RTILs),²⁵ the dynoles,²⁶ and the dimeric tyrphostins, exemplified by bis-tyrphostin (Bis-T).^{27,28} Other groups have reported dynastore²⁹ and some selective serotonin reuptake inhibitors.³⁰ Inhibitors from all laboratories to date exhibit low micromolar potency. On the basis of our knowledge of the Bis-T pharmacophore, herein we report on a new series of dynamin inhibitors based on iminochromenes (“iminodys”, iminochromene based dynamin inhibitors) that are the first nanomolar potent inhibitors of dynamin yet reported.

Results

Our previous studies in developing dimeric tyrphostins suggested a highly prescribed pharmacophore in which little structural modifications were permissible. The most promising inhibitor in our previous study was 2-cyano-*N*-{3-[2-cyano-3-(3,4,5-trihydroxyphenyl)acryloylamino]ethyl}-3-(3,4,5-trihydroxyphenyl)acrylamide (Bis-T-22, **1** $\text{IC}_{50} = 1.7 \pm 0.2 \mu\text{M}$; see Figure 1).²⁷ Attempts to introduce variations in the central alkyl linker only resulted in a complete loss of activity. Bioisosteric replacement of the amide linker with the corresponding ester effected a 10- to 50-fold decrease in inhibition.²⁷ Methylation of the amide NH (*N*-CH₃ either mono or bis variants) resulted in a similar loss of potency. We also noted an ablation of activity on removal of the nitrile moieties. In our earlier structure–activity relationship (SAR) report we had also established the pivotal nature of the catechol units. More recently, we explored the development of a new series of asymmetric Bis-T analogues with a focus on developing potential photoaffinity labeling groups to facilitate a greater understanding of Bis-T’s binding interactions with dynamin.²⁸ Typically, these efforts revealed that complete removal of the catechol moiety was detrimental to dynamin I activity with a 100-fold decrease in inhibition. Analogues bearing a single oxygen containing moiety returned a modest level of dynamin inhibition but still 25-fold less than that of the parent Bis-T. Interestingly both photoaffinity labeling analogues displayed modest and excellent dynamin inhibition (Figure 1).²⁸

While our prior studies clearly demonstrated that the removal of the nitrile moiety was detrimental to activity, we proposed that the development of an isosteric replacement was feasible. The nitrile itself may play a number of key roles in Bis-T binding to dynamin I. First, it may be directly involved in enzyme binding through a hydrogen or dipole–dipole bonding interaction or alternatively in mediating the

Scheme 1^a



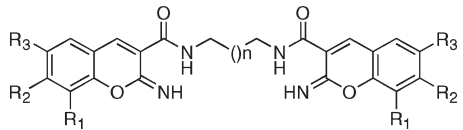
^a Reagents and conditions for generation of the iminodys: (i) ethanol, piperidine (cat.), reflux 2 h.

optimal position of key functional groups within the active site. In light of these considerations we turned our attention to exploring the effect of placing alternative functional groups in this position. Additionally, nitrile free tyrphostin analogues are known to be poor epidermal growth factor receptor (EGFR) tyrosine kinase inhibitors.³¹ Therefore, we were keen to remove the nitrile groups and to introduce a more druglike isostere, expanding the repertoire of analogues inhibiting the GTPase activity of dynamin I. We believed that rapid development of the above pharmacophore would be possible by commencing our synthesis with a family of 2-hydroxybenzaldehydes.³² Utilizing our Knoevenagel approaches and α,ω -bis-cyanoamides would generate the corresponding series of iminodys (Scheme 1).^{29,33–35} These iminodys analogues would maintain the required free amide-NH and aromatic moieties but would introduce a second ring (in turn increasing the conformational rigidity of these analogues) and an imine moiety at the expense of the 2-OH and the undesired nitriles.

Thus, treatment of a family of 2-hydroxybenzaldehydes (**7–12**) with α,ω -biscyanoamides (**13a–e**) under standard Knoevenagel condensation conditions afforded the desired analogues (**14–38**) in good to excellent yield (48–88%) (Scheme 1).^{27,33–35} The results of screening for inhibition of dynamin I GTPase activity are shown in Table 1.

The synthesis and biological evaluation of five libraries of iminodys (each library being based on the length of the central alkyl linker: $n = 0, 1, 2, 3$, and 4) afforded 13 active analogues from a library of 25 (Table 1, **16–18, 20–23, 27, 28, 32, 33, 37**, and **38**). As anticipated from prior results with dimeric tyrphostins,²⁷ analogues lacking at least one –OH moiety (**14, 19, 24, 29**, and **34**) were inactive ($\text{IC}_{50} > 300 \mu\text{M}$). To our surprise the monohydroxylated analogues **16, 20**, and **21** returned IC_{50} values of $\sim 100, 36.6$, and $17.3 \mu\text{M}$, respectively. In the corresponding dimeric tyrphostin analogues no activity was detected even at concentrations of $> 300 \mu\text{M}$.²⁷

Analogues with two adjacent –OH moieties typically displayed the highest-level inhibition; e.g., **18, 27**, and **28** are all low micromolar potent ($\text{IC}_{50} < 10 \mu\text{M}$), with **17, 22**, and **23** being the first nanomolar potent dynamin inhibitors reported returning IC_{50} values of $330 \pm 70, 450 \pm 50$, and $260 \pm 80 \text{ nM}$, respectively. In our in vitro studies there was no discernible preference for a 6,7- or 7,8-OH disposition noted. Extension of the central alkyl linker had little effect with $n = 0–2$; however, with $n = 3$, a 5-fold decrease (**32, 33** IC_{50} values of 19 ± 2 and $17 \pm 2 \mu\text{M}$, respectively) in activity was observed, and with $n = 4$, a 20-fold decrease (**37, 38** IC_{50} values of 70 ± 10 and $82 \pm 13 \mu\text{M}$, respectively) in activity was observed

Table 1. Inhibition of Dynamin I GTPase Activity by Iminodins **16**–**40**


compd	R ₁	R ₂	R ₃	alkyl linker, <i>n</i>	IC ₅₀ (μM) ^a
14	H	H	H	0	<i>b</i>
15	OH	H	H	0	<i>b</i>
16	H	OH	H	0	100 ^c
17	OH	OH	H	0	0.33 ± 0.07
18	H	OH	OH	0	6.0 ± 2.2
19	H	H	H	1	<i>b</i>
20	OH	H	H	1	36.6 ± 7.2
21	H	OH	H	1	17.3 ± 1.0
22	OH	OH	H	1	0.45 ± 0.05
23	H	OH	OH	1	0.26 ± 0.08
24	H	H	H	2	<i>b</i>
25	OH	H	H	2	<i>b</i>
26	H	OH	H	2	<i>b</i>
27	OH	OH	H	2	4.3 ± 2.7
28	H	OH	OH	2	3.2 ± 2.2
29	H	H	H	3	<i>b</i>
30	OH	H	H	3	<i>b</i>
31	H	OH	H	3	<i>b</i>
32	OH	OH	H	3	19 ± 2
33	H	OH	OH	3	17 ± 2
34	H	H	H	4	<i>b</i>
35	OH	H	H	4	<i>b</i>
36	H	OH	H	4	<i>b</i>
37	OH	OH	H	4	70 ± 10
38	H	OH	OH	4	82 ± 13

^a IC₅₀ determinations are the mean ± 95% confidence interval (CI) of a single experiment performed in triplicate. ^b About 50% inhibition at 100 μM drug concentrations. Full IC₅₀ determination not conducted. ^c No inhibition at 300 μM drug concentration.

(Table 1). This is analogous to our previous findings with the linker length in Bis-T analogues.²⁷

The retention of activity in the absence of the free –CN with the iminodyn derivatives was unexpected but desired, as our previous studies have shown that their removal renders the corresponding dimeric tyrphostins inactive. This represents the first bioisosteric modification of the Bis-T skeleton while maintaining inhibition of dynamin I GTPase activity and extends the Bis-T pharmacophore.

Given that dynamin is essential for endocytosis, we next determined the ability of our five most potent iminodins, **17** and **20**–**23**, for in-cell activity (Figure 2). First we examined their ability to block RME of Texas Red-Tf (Tf-TxR) in human bone osteosarcoma epithelial cells (U2OS). To quantify the effect of iminodyn analogues **17** and **20**–**23** in these cells, we used our previously reported automated quantitative RME assay based on endocytosis of Tf-TxR. Tf-TxR binds to the transferrin receptor and is internalized by a dynamin II-dependent pathway.²⁴ After a 30 min preincubation in the presence of increasing concentrations of iminodins **17** and **20**–**23**, RME was greatly reduced (Table 2). Iminodyn-**22** was the most potent RME inhibitor, returning an IC₅₀ of 10.7 ± 4.5 μM, making it among the most potent RME inhibitors yet reported, comparable to dynole 34-2.²⁶ It was clear that **17** and **20**–**23** greatly differ in their ability to block RME, with only **20** and **22** returning significant activity. Surprisingly, neither **17** nor **21** exhibited any in-cell activity. Importantly cell morphology was unaffected by the treatment with **20**, **22**,

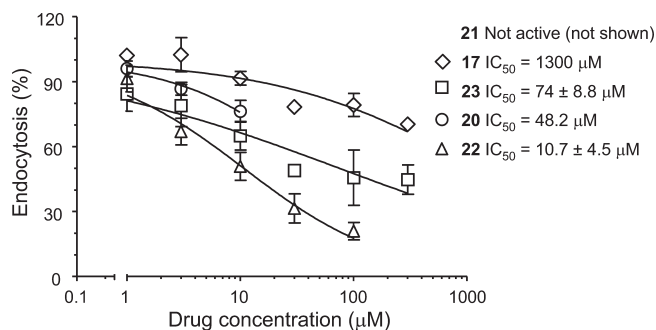


Figure 2. IC₅₀ curves for endocytosis block in U2OS cells of iminodyn analogues **17** and **20**–**23**. U2OS cells were preincubated with vehicle only or with different iminodins for 30 min and then incubated with Tf-TxR (A1) for 8 min. Data are the mean fluorescence as a percent of control cells (triplicate determinations on approximately 1200 cells each) ± SEM. The results are representative of three independent experiments.

or **23**, even after 30 min of exposure (data not shown), indicating that there was no membrane disruption. In previous studies we have noted that the inhibition of RME has often followed the same rank order of potency shown with our in vitro evaluations. However, with the analogous studies here, this was not the case. As can be seen in Table 2, there is no direct correlation of dynamin I in vitro inhibition with the observed RME inhibition.

Of all the data acquired in the evaluation of RME inhibition, the contrast between iminodyn-**17** and iminodyn-**22** is striking. Both are nanomolar dynamin I inhibitors, differing only by a single methylene in the alkyl linker (**17** is ethyl; **22** is propyl). Iminodyn-**17** is a 330 nM dynamin I inhibitor but a ~1300 μM inhibitor of RME, compared with **22** which is a 450 nM dynamin I inhibitor but a 10.7 μM inhibitor of RME. With the other iminodins examined for their ability to block RME we note that the position of the single –OH moiety with **19** and **20** is crucial for activity against RME with only the 7-OH (**20**) displaying any noteworthy level of RME block (IC₅₀ = 48.2 μM). A similar positional dependency is also apparent on comparison of the 7,8- and 6,7- dihydroxy analogues **22** and **23**, with the position of the second –OH moiety important for the level of RME block observed (IC₅₀ = 10.7 ± 4.5 vs 74.6 ± 8.8 μM, respectively).

Given that RME is a dynamin II mediated process, it appears as though **17** might display a high level of dynamin I specificity. As the RME assay is a whole cell assay and consequently does not directly reflect the level of dynamin II inhibition, we examined the effect of **17** and **22** on the inhibition of dynamin II GTPase activity. While dynamin I in this study was the endogenous form purified from sheep brain, dynamin II was produced as a recombinant protein expressed in Sf9 insect cells. Subtle differences between the dynamin I and dynamin II assay conditions mean that the data are indicative only, with differing dynamin and lipid concentrations being required for each assay. Notwithstanding this caveat, we obtained dynamin II IC₅₀ curves for all five iminodins in Table 2. All returned IC₅₀ values were essentially indistinguishable from that of dynamin I, suggesting that these compounds have no selectivity between the two dynamin forms.

With these data in hand we can see that with iminodyn-**17** there is a 4000-fold change in activity for isolated dynamin II and dynamin II mediated RME, whereas with iminodyn-**22**

Table 2. Inhibition of Dynamin I and Dynamin II in Vitro GTPase Activity and In-Cell Receptor Mediated Endocytosis (RME) and Synaptic Vesicle Endocytosis (SVE) by Iminodins **17** and **20–23**

Iminodyn Compound	Iminodyn Structure	Dyn I GTPase activity	Dyn II GTPase activity	RME (Tf uptake in U2OS cells)	SVE (FM4-64 uptake in synaptosomes)
		IC ₅₀ (μM) ^[a]	IC ₅₀ (μM) ^[b]	IC ₅₀ (μM) ^[b]	IC ₅₀ (μM) ^[b]
17		0.33 ± 0.07	0.44 ± 0.19	1300	Not active
20		36.6 ± 7.2	34.8 ± 5.6	48.2	Not active
21		17.3 ± 1.0	16.7 ± 3.6	Not active	66.1 ± 2.1
22		0.45 ± 0.05	0.39 ± 0.15	10.7 ± 4.5	99.5 ± 1.7
23		0.26 ± 0.08	0.29 ± 0.11	74.6 ± 8.8	40.4 ± 0.8

^aIC₅₀ determinations are the average of at least two independent experiments, each in triplicate. ^bMean ± 95% confidence interval (CI) of a single experiment performed in triplicate.

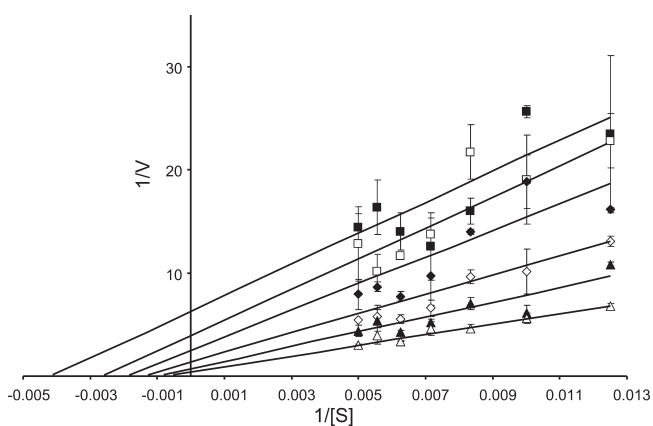


Figure 3. Uncompetitive kinetics of iminodyn-22 with respect to GTP. The data depict iminodyn-22 concentration dependent changes in a double-reciprocal plot between substrate (GTP at 80–200 μM) and velocity. The data correspond to iminodyn-22 concentrations at 1.2 (■) 1.1 (□), 1.0 (◆), 0.9 (◇), 0.8 (▲), and 0.7 (△) μM. Error bars represent the mean ± SEM of three independent experiments each conducted in triplicate.

there is only a 24-fold decrease. Logically this change is primarily effected by the difference in the number of methylene units in the spacer chain, with the ethyl linker affording a more prescriptive orientation that appears to be unfavorable to cell penetration. Interestingly, we did not note any such effect with the corresponding Bis-T analogue (data not shown); presumably this is an effect of the increased conformational rigidity afforded to iminodyn-17 by tethering of the “cyanoamide moiety” as the fused iminochromene ring.

As SVE is a dynamin I mediated process, we next examined the ability of key analogues to inhibit SVE. We used isolated rat brain nerve terminals (synaptosomes) and imaged the uptake of the styryl dye FM4-64 by endocytosis, a well characterized endocytic marker in this system.³⁶ We note that the

concentration of dynamin I in synaptosomes is approximately 50-fold higher than that of dynamin II.³⁷ Iminodins **21**, **22**, and **23** showed significant inhibition of SVE, while iminodyn-17 had no activity as found for RME (Table 2). The results are consistent with the ability of the iminodins to inhibit both dynamins in cells where the compounds can access the cell interior.

Finally, to explore the mechanism of inhibition of the iminodins on dynamin I, we conducted a series of Michaelis–Menten kinetic experiments with iminodyn-22 (0.7–1.2 μM) and varying concentrations of the Mg²⁺·GTP substrate (80–200 μM). The Lineweaver–Burke plots demonstrate parallel double-reciprocal plots corresponding to different concentrations of iminodyn-22, suggesting that iminodyn-22 is most likely to be an uncompetitive inhibitor of dynamin I (Figure 3).

Conclusions

Herein we have developed a new chemical class of dynamins I and II GTPase inhibitors based on an iminochromene scaffold. We call these new classes of dynamin inhibitors the iminodins. They are the first reported nanomolar potent dynamin inhibitors. The most potent of these were iminodyn-17 (IC₅₀ = 330 ± 70 nM), iminodyn-22 (IC₅₀ = 450 ± 50 nM), and iminodyn-23 (IC₅₀ = 260 ± 80 nM), which are about 5-fold more potent than our previously reported dynoles (dynole 34-2 IC₅₀ = 1.30 ± 0.30 μM)²⁶ and are over 400 times more potent than dynasore (IC₅₀ ≈ 15 μM).²⁹ These analogues bind to the GTPase domain and exert their influence on dynamin via a mechanism that is uncompetitive with GTP binding. SAR reveals similarities and surprising differences from those previously determined for dimeric tyrosphostins.^{27,28} The iminodins have allowed the incorporation of Bis-T’s cyano moieties as imines exocyclic to a second fused ring, showing for the first time that removal of the cyano moieties of Bis-T is feasible, and indeed with the iminodins improves activity. The introduction of a second, fused ring is a

new pharmacophore that reveals that while there was no observable difference in dynamin IC_{50} with the 6,7- or 7,8-dihydroxy analogues **22** and **23**, there was a preference with RME block for an $-OH$ moiety to be at C7. Another feature not observed with the Bis-T series is the retention of some degree of dynamin inhibition with the monohydroxylated **16**, **20**, and **21** (all IC_{50} values of $<100 \mu M$). Finally, the ethyl linked iminodyn-**17** displayed no RME block ($IC_{50} \approx 1300 \mu M$), whereas the propyl linked iminodyn-**22** returned the best RME block ($IC_{50} = 10.7 \pm 4.5 \mu M$). Such differentiation was not apparent in the Bis-T series. Thus, this work has expanded the dynamin pharmacophore associated with the Bis-T, and now iminodyn, series of compounds.

Several of the lead iminodyns were effective in the cell-based inhibition of RME and SVE. In particular, iminodyn-**22** showed the most promise as a broad spectrum, general purpose dynamin inhibitor that does not discriminate between dynamin I and dynamin II and that potently inhibits cellular RME. Iminodyn-**22** is about half as potent as dynole 34-2 and is about 8-fold more potent than dynasore, making it an effective tool for the study of cellular endocytosis in a broad variety of systems. The ability of iminodyn-**22** to also inhibit SVE is likely a reflection of its dual specificity on dynamins I and II. Because of the diversity of cellular systems regulated by the dynamins, these compounds should be evaluated in the future for potential clinical applications in a variety of disorders ranging from cancer to pathogen infection.

Experimental Section

Biology. Materials. Phosphatidylserine (PS), phenylmethylsulfonyl fluoride (PMSF), and Tween-80 were from Sigma-Aldrich (St. Louis, MO). GTP was from Roche Applied Science (Germany), leupeptin was from Bachem (Bubendorf, Switzerland). Gel electrophoresis reagents, equipment, and protein molecular weight markers were from Bio-Rad (Hercules, CA). Collagenase was from Roche. Paraformaldehyde (PFA) was from Merck Pty Ltd. (Kilsyth, Australia). Coverslips were from Lomb Scientific (Sydney, Australia). Penicillin/streptomycin, phosphate buffered salts, fetal calf serum (FCS), Grace's insect cell media, and Dulbecco's Modified Eagle's Medium (DMEM) were from Invitrogen (Mount Waverley, Victoria, Australia). Alexa-594 conjugated Tf (Tf-A594) and DAPI were from Molecular Probes (OR). Polyethylenimine was from Polysciences Inc. (Warrington, PA). All other reagents were of analytical reagent grade or better.

Drugs. Drugs were synthesized in-house and made up as stock solutions in 100% DMSO and diluted in 50% v/v DMSO/20 mM Tris-HCl, pH 7.4, or cell media prior to further dilution in the assay. The final DMSO concentration in the GTPase or endocytosis assays was at most 3.3% or 1%, respectively. The GTPase assay for dynamin I was unaffected by DMSO up to 3.3%. Drugs were dissolved as 30 mM stocks in 100% DMSO and were light-yellow in color. Stocks were stable and could be stored at $-20^\circ C$ for several months. They were diluted into solutions of 50% DMSO made up in 20 mM Tris-HCl, pH 7.4, and then diluted again into the final assay.

Protein Production. Endogenous dynamin I was purified from sheep brain by extraction from the peripheral membrane fraction of whole brain³⁸ and affinity purification on GST-Amph2-SH3-sepharose as described,³⁹ yielding 8–10 mg of protein from 250 g of sheep brain. Dynamin II (His-6-tagged) DNA inserted into the pIEx-6 vector was generously provided by Sandra Schmid and Sylvia Neumann (The Scripps Research Institute). The plasmid was used to transfect Sf9 insect cells using polyethylenimine as the transfection reagent using a DNA/polyethylenimine ratio of 1:5 for 48 h.⁴⁰ Following transfection, the cells were harvested and lysed, and overexpressed dynamin II was purified using GST-Amph2-SH3-sepharose as described

above for dynamin I. The yield from 1 L of insect cell suspension culture (1×10^6 cells/mL) was typically 1–2 mg of protein with greater than 98% purity.

Malachite Green GTPase Assay. The Malachite Green method was used for the sensitive colorimetric detection of orthophosphate (P_i). It is based on the formation of a phosphomolybdate complex at low pH with basic dyes, causing a color change. The assay procedure is based on stimulation of native sheep brain-purified dynamin I by sonicated phosphatidylserine (PS) liposomes.⁴¹ However, in our earlier studies with Bis-T we used 200 nM dynamin I while in the present study we used 20 nM, requiring a reformulation of assay volumes and the Malachite Green reagent for the present study.^{23,27,39} Purified dynamin I (20 nM) (diluted in 6 mM Tris-HCl, 20 mM NaCl, 0.01% Tween-80, pH 7.4) was incubated in GTPase assay buffer (5 mM Tris-HCl, 10 mM NaCl, 2 mM Mg^{2+} , 0.05% Tween-80, pH 7.4, 1 $\mu g/mL$ leupeptin, and 0.1 mM PMSF) with 0.3 mM GTP in the presence of test compound for 30 min at $37^\circ C$. The final assay volume was 150 μL in round bottomed 96-well plates. Plate incubations were performed in a dry heating block with shaking at 600 rpm (Eppendorf Thermomixer). Dynamin I GTPase activity was maximally stimulated by addition of 4 $\mu g/mL$ PS liposomes (although this concentration slightly varies from batch to batch of dynamin I). For dynamin II GTPase assay, higher concentrations of dynamin II (69 nM) were used with 25 $\mu g/mL$ PS being required for its activity to be maximally stimulated. Dynamin II was preincubated with PS for 10 min at room temperature (in 6 mM Tris-HCl, 20 mM NaCl, 0.01% Tween-80, pH 7.4), following which the mixture was incubated in GTPase assay buffer (5 mM Tris-HCl, 10 mM NaCl, 2 mM Mg^{2+} , 0.05% Tween-80, pH 7.4, 1 $\mu g/mL$ leupeptin, and 0.1 mM PMSF) with 0.3 mM GTP in the presence of test compound for 30 min at $37^\circ C$. Dynamin I did not require preincubation with PS. The final assay volume and the shaking conditions were the same for both dynamins I and II GTPase assays. The reactions were all terminated with 10 μL of 0.5 M EDTA, pH 8.0, and the samples were stable for several hours at room temperature. To each well was added 40 μL of Malachite Green solution (2% w/v ammonium molybdate tetrahydrate, 0.15% w/v malachite green, and 4 M HCl; the solution was passed through 0.45 μm filters and stored in the dark for up to 2 months at room temperature), and color was allowed to develop for 5 min (and was stable up to 2 h). The absorbance of samples in each plate was determined on a microplate spectrophotometer at 650 nm. Phosphate release was quantified by comparison with a standard curve of sodium dihydrogen orthophosphate monohydrate (baked dry at $110^\circ C$ overnight) which was run in each experiment. GraphPad Prism 5 (GraphPad Software Inc., San Diego, CA) was used for plotting data points and analysis of enzyme kinetics using nonlinear regression. Dynamin I GTPase data are reported as basal activity subtracted from PS-stimulated activity. Dynamin II GTPase data are reported as maximal stimulated activity. The maximum GTPase activity was titrated to be the same for both enzymes. These assays can also be conducted in the absence of Tween with little effect on the IC_{50} values noted for the iminodyns listed in Figure 1.

Kinetic Analysis of Iminodyn-22 in Competition with Mg^{2+} -GTP. Dynamin I at a final concentration of 11 nM was incubated with GTPase buffer containing phosphatidylserine (4 $\mu g/mL$) and varying amounts of GTP (80–200 μM) in the presence of IC-**22** at a concentration range of 0.7–1.2 μM . The reaction was stopped after 30 min by addition of EDTA (0.5 mM, pH 7.4). Curves were generated using the Michaelis–Menten equation $v = V_{max}[S]/(K_m + [S])$ where S = PS activator or GTP substrate. After the V_{max} and K_m values were determined, the data were transformed using the Lineweaver–Burke equation, $1/v = 1/V_{max} + (K_m/V_{max})(1/[S])$.

Texas Red-Tfn Uptake. U2OS cells were cultured in DMEM supplemented with 10% FCS at $37^\circ C$ and in 5% CO_2 in a

humidified incubator. Tf uptake was analyzed on the basis of methods previously described.^{42,43} Briefly, cells were grown in fibronectin-coated (5 $\mu\text{g}/\text{mL}$) 96-well plates. The cells were serum-starved overnight (16 h) in DMEM minus FCS. Cells were then incubated with iminodins **17** and **20–23** (usually 30 μM) or vehicle for 30 min prior to addition of 4 $\mu\text{g}/\text{mL}$ Tf-TxR for 8 min at 37 °C. Cell-surface-bound Tf was removed by incubating the cells in an ice cold acid wash solution (0.2 M acetic acid + 0.5 M NaCl, pH 2.8) for 10 min and was with ice cold PBS for 5 min. Cells were immediately fixed with 4% PFA for 10 min at 37 °C. Nuclei were stained using DAPI. Quantitative analysis of the inhibition of Tf-TxR endocytosis in U2OS cells was performed on large numbers of cells by an automated acquisition and analysis system (ImageXpress Micro (IXM), Molecular Devices, Sunnyvale, CA). Nine images were collected from each well, averaging 40–50 cells per image. The average integrated intensity of Tf-TxR signal per cell was calculated for each well using IXM system, and the data were expressed as a percentage of control cells (vehicle treated). The average number of cells for each data point was ~ 1200 . IC₅₀ values were calculated using Graphpad Prism, version 5, and data were expressed as the mean \pm 95% confidence interval (CI) for three wells and ~ 1200 cells.

FM 4-64 Assay of Synaptic Vesicle Endocytosis. Highly purified synaptosomes were prepared from the cerebrum of adult male Sprague–Dawley rats, as described.⁴⁴ Synaptosomes were attached to 96-well glass-bottom plates at 4 °C. Synaptosomes were maintained at 30 °C in a physiological saline buffer (143 mM NaCl, 4.7 mM KCl, 20 mM 4-(2-hydroxyethyl)-1-piperazineethanesulfonic acid (HEPES), 1.2 mM MgSO₄, 0.1 mM CaCl₂, pH 7.4). Once attached, synaptosomes were incubated in buffer containing either DMSO alone (control) or drug dissolved in DMSO. DMSO was kept at a concentration of 1% in all samples. Drug incubation was carried out for 30 min. The synaptosomes were then exposed to 1 μM *N*-(3-triethylammoniumpropyl)-4-(4-diethylaminophenyl)hexatrienyl)pyridinium dibromide (FM 4-64) (Invitrogen) in the presence of drug for 2 min. Synaptosomes were then depolarized in 80 mM KCl for a further 2 min to induce exocytosis/endocytosis, thereby facilitating uptake of FM 4-64. After depolarization, synaptosomes were returned to standard physiological saline buffer. Fluorescent images of synaptosomes were acquired using the IXM system with a 20 \times air objective at excitation 476–524 nm and emission at 608–742 nm emission. Images were analyzed using MetaXpress software.

Chemistry. General Methods. All solvents were bulk quality and redistilled prior to use. Flash chromatography was carried out using silica gel 200–400 mesh (60 Å). ¹H and ¹³C NMR were recorded at 300 and 75 MHz, respectively, using a Bruker Avance 300 MHz spectrometer in CDCl₃ and DMSO-*d*₆. GCMS was performed using a Shimadzu GCMS-QP2100. The instrument uses a quadrupole mass spectrometer and detects samples via electron impact ionization (EI). The Biomolecular Mass Spectrometry Laboratory of the University of Wollongong, Australia, analyzed samples for HRMS. The spectra were run on the VG Autospec-oe-tof tandem high resolution mass spectrometer using CI (chemical ionization), with methane as the carrier gas and PFK (perfluorokerosene) as the reference. Microanalysis was conducted at the Microanalysis Unit at the Australian National University, Canberra, Australia. Compound purity was confirmed by a combination of LC–MS (HPLC), micro and/or high resolution mass spectrometry and NMR analysis. All analogues are $\geq 95\%$ purity.

Synthesis of the Cyanoamide Linker Units (13a–e). The synthesis of *N,N*-(ethane-1,2-diyl)bis(2-cyanoacetamide) (**13a**), *N,N*-(propane-1,2-diyl)bis(2-cyanoacetamide) (**13b**), *N,N*-(butane-1,2-diyl)bis(2-cyanoacetamide) (**13c**), *N,N*-(pentane-1,2-diyl)bis(2-cyanoacetamide) (**13d**), and *N,N*-(hexane-1,2-diyl)bis(2-cyanoacetamide) (**13e**) have been reported previously.²⁷

***N,N'*-(Ethane-1,2-diyl)bis(2-imino-2*H*-chromene-3-carboxamide) (14).** *N,N'*-(Ethane-1,2-diyl)bis(2-cyanoacetamide) (**13a**) (0.194 g, 1 mmol), 2-hydroxybenzaldehyde (0.244 g, 2 mmol), 3 drops of piperidine, and ethanol (10 mL) were heated at reflux for 2 h. Cooling, filtering, and washing with cold ether gave, after recrystallization from ethanol, an off-white solid: 0.261 g (65%); mp 293–295 °C. ¹H NMR (DMSO-*d*₆): 3.48 (4H, br s), 7.23 (4H, m), 7.52 (2H, m), 7.75 (2H, m), 8.39 (2H, s), 8.93 (2H, s), 10.43 (2H, br s). ¹³C NMR (DMSO-*d*₆): 38.7, 115.2, 119.7, 120.7, 124.4, 130.3, 133.3, 141.1, 153.9, 155.7, 162.2. C₂₂H₁₈N₄O₄ calculated: C, 65.66; H, 4.51; N, 13.92. Found: C, 65.84; H, 4.31; N, 14.05.

***N,N'*-(Ethane-1,2-diyl)bis(8-hydroxy-2-imino-2*H*-chromene-3-carboxamide) (15).** Iminodyn-**15** was prepared in a similar manner to the synthesis of **14**, from *N,N'*-(ethane-1,2-diyl)bis(2-cyanoacetamide) (**13a**) and 2,3-dihydroxybenzaldehyde (2 equiv) to give, after recrystallization from ethanol, an off-white solid (64%): mp > 300 °C. ¹H NMR (DMSO-*d*₆): 3.47 (4H, br m), 7.04 (4H, s), 7.14 (2H, br m), 8.34 (2H, br m), 8.77 (2H, br), 10.48 (2H, br s). ¹³C NMR (DMSO-*d*₆): 38.8, 119.2, 119.7, 119.9, 123.8, 141.8, 143.8, 145.8, 146.1, 155.5, 161.4. C₂₂H₁₈N₄O₆ calculated: C, 60.83; H, 4.18; N, 12.90. Found: C, 61.03; H, 4.15; N, 12.75.

***N,N'*-(Ethane-1,2-diyl)bis(7-hydroxy-2-imino-2*H*-chromene-3-carboxamide) (16).** Iminodyn-**16** was prepared in a similar manner to the synthesis of **14**, from *N,N'*-(ethane-1,2-diyl)bis(2-cyanoacetamide) (**13a**) and 2,4-dihydroxybenzaldehyde (2 equiv) to give, after recrystallization from ethanol, an off-white solid (74%): mp 283–285 °C. ¹H NMR (DMSO-*d*₆): 3.49 (4H, br m), 7.00–7.18 (6H, m), 7.62 (1H, br m), 8.29 (2H, s), 9.38 (2H, br s), 10.20 (2H, br s). ¹³C NMR (DMSO-*d*₆): 38.7, 119.9, 120.2, 124.2, 140.1, 142.3, 145.7, 149.2, 157.3, 163.4. C₂₂H₁₈N₄O₆ calculated: C, 60.83; H, 4.18; N, 12.90. Found: C, 60.79; H, 4.35; N, 13.72.

***N,N'*-(Ethane-1,2-diyl)bis(7,8-dihydroxy-2-imino-2*H*-chromene-3-carboxamide) (17).** Iminodyn-**17** was prepared in a similar manner to the synthesis of **14**, from *N,N'*-(ethane-1,2-diyl)bis(2-cyanoacetamide) (**13a**) and 2,3,4-trihydroxybenzaldehyde (2 equiv) to give, after recrystallization from ethanol, a red solid (82%): mp > 300 °C. ¹H NMR (DMSO-*d*₆): 3.50 (4H, br m), 6.67 (2H, d, *J* = 8.4 Hz), 7.03 (2H, d, *J* = 8.5 Hz), 7.65 (2H, br m), 8.25 (2H, s), 9.30 (2H, br s). ¹³C NMR (DMSO-*d*₆): 39.0, 118.2, 119.7, 120.1, 126.2, 140.1, 142.3, 148.4, 150.1, 158.1, 165.1. HRMS: calculated for C₂₃H₂₀N₄O₄ 417.1563. Found (ESI⁺) (M + H) 417.1563.

***N,N'*-(Ethane-1,2-diyl)bis(6,7-dihydroxy-2-imino-2*H*-chromene-3-carboxamide) (18).** Iminodyn-**18** was prepared in a similar manner to the synthesis of **14**, from *N,N'*-(ethane-1,2-diyl)bis(2-cyanoacetamide) (**13a**) and 2,4,5-trihydroxybenzaldehyde (2 equiv) to give, after recrystallization from ethanol, a dark-green solid (72%): mp > 300 °C. ¹H NMR (DMSO-*d*₆): 3.50 (4H, br m), 7.12 (2H, s), 7.23 (2H, s), 7.84 (2H, br m), 9.03 (2H, s), 9.25 (2H, br s). ¹³C NMR (DMSO-*d*₆): 37.8, 118.2, 119.1, 119.9, 124.2, 141.2, 146.3, 154.2, 156.1, 163.2. C₂₂H₁₈N₄O₈ calculated: C, 56.65; H, 3.89; N, 12.01. Found: C, 57.00; H, 4.09; N, 12.71.

***N,N'*-(Propane-1,3-diyl)bis(2-imino-2*H*-chromene-3-carboxamide) (19).** Iminodyn-**19** was prepared in a similar manner to the synthesis of **14**, from *N,N'*-(propane-1,2-diyl)bis(2-cyanoacetamide) (**13b**) and 2-hydroxybenzaldehyde (2 equiv) to give, after recrystallization from ethanol, a yellow solid (62%): mp 253–255 °C. ¹H NMR (DMSO-*d*₆): 1.72 (2H, br m), 3.51 (4H, br m), 7.22 (4H, m), 7.50 (2H, m), 7.73 (2H, m), 8.42 (2H, s), 8.88 (2H, s), 10.40 (2H, br s). ¹³C NMR (DMSO-*d*₆): 29.3, 37.9, 115.1, 119.4, 121.1, 125.6, 130.5, 134.1, 140.0, 152.1, 156.2, 164.1. C₂₃H₂₀N₄O₄ calculated: HRMS (ESI⁺) (M + H) 417.1563. Found 417.1563.

***N,N'*-(Propane-1,3-diyl)bis(8-hydroxy-2-imino-2*H*-chromene-3-carboxamide) (20).** Iminodyn-**20** was prepared in a similar manner to the synthesis of **14**, from *N,N'*-(propane-1,2-diyl)bis(2-cyanoacetamide) (**13b**) and 2,3-dihydroxybenzaldehyde

(2 equiv) to give, after recrystallization from ethanol, a light-yellow solid (73%): mp 274–276 °C. ¹H NMR (DMSO-*d*₆): 1.74 (2H, br s), 3.48 (4H, br s), 6.99 (4H, s), 7.19 (2H, br m), 8.43 (2H, br m), 8.82 (2H, br m), 10.45 (2H, br s). ¹³C NMR (DMSO-*d*₆): 28.2, 37.3, 110.2, 118.9, 120.1, 122.9, 141.0, 141.2, 142.8, 145.8, 156.3, 162.3. C₂₃H₂₀N₄O₆ calculated: C, 61.60; H, 4.50; N, 12.49. Found: C, 61.25; H, 4.65; N, 12.69.

***N,N'*-(Propane-1,3-diyl)bis(7-hydroxy-2-imino-2*H*-chromene-3-carboxamide) (21).** Iminodyn-21 was prepared in a similar manner to the synthesis of **14**, from *N,N'*-(propane-1,2-diyl)-bis(2-cyanoacetamide) (**13b**) and 2,4-dihydroxybenzaldehyde (2 equiv) to give, after recrystallization from ethanol, an off white solid (51%): mp 288–290 °C. ¹H NMR (DMSO-*d*₆): 1.74 (2H, br s), 3.35 (4H, br s), 7.00–7.18 (6H, m), 7.61 (1H, br m), 8.30 (2H, s), 9.41 (2H, br s), 10.23 (2H, br s). ¹³C NMR (DMSO-*d*₆): 28.4, 38.2, 118.1, 119.5, 119.9, 123.1, 141.2, 142.3, 146.3, 150.4, 156.1, 164.2. HRMS: calculated for C₂₃H₂₀N₄O₆ 448.1383. Found (ESI⁺) (M + H) 448.1382.

***N,N'*-(Propane-1,3-diyl)bis(7,8-dihydroxy-2-imino-2*H*-chromene-3-carboxamide) (22).** Iminodyn-22 was prepared in a similar manner to the synthesis of **14**, from *N,N'*-(propane-1,2-diyl)-bis(2-cyanoacetamide) (**13b**) and 2,3,4-trihydroxybenzaldehyde (2 equiv) to give, after recrystallization from ethanol, a red solid (69%): mp > 300 °C. ¹H NMR (DMSO-*d*₆): 1.72 (2H, br m), 3.40 (4H, br m), 6.63 (2H, d, *J* = 8.4 Hz), 6.94 (2H, d, *J* = 8.5 Hz), 7.62 (2H, br s), 8.32 (2H, s), 9.31 (2H, br m). ¹³C NMR (DMSO-*d*₆): 28.2, 39.0, 118.2, 119.7, 120.1, 126.2, 140.1, 142.3, 148.4, 150.1, 158.1, 165.1. HRMS: calculated for C₂₃H₂₀N₄O₈ 481.1359. Found (ESI⁺) (M + H) 481.1355.

***N,N'*-(Propane-1,3-diyl)bis(6,7-dihydroxy-2-imino-2*H*-chromene-3-carboxamide) (23).** Iminodyn-23 was prepared in a similar manner to the synthesis of **14**, from *N,N'*-(propane-1,2-diyl)-bis(2-cyanoacetamide) (**13b**) and 2,4,5-trihydroxybenzaldehyde (2 equiv) to give, after recrystallization from ethanol, a dark-green solid (64%): mp 262–263 °C. ¹H NMR (DMSO-*d*₆): 1.75 (2H, br m), 3.51 (4H, br s), 7.00 (2H, s), 7.30 (2H, s), 7.85 (2H, br m), 9.01 (2H, s), 9.22 (2H, br s). ¹³C NMR (DMSO-*d*₆): 27.2, 37.6, 118.1, 119.4, 119.9, 125.8, 139.3, 140.2, 147.2, 155.0, 157.2, 166.1. HRMS: calculated for C₂₃H₂₀N₄O₈ 481.1359. Found (ESI⁺) (M + H) 481.1347.

***N,N'*-(Butane-1,3-diyl)bis(2-imino-2*H*-chromene-3-carboxamide) (24).** Iminodyn-24 was prepared in a similar manner to the synthesis of **14**, from *N,N'*-(butane-1,2-diyl)-bis(2-cyanoacetamide) (**13c**) and 2-hydroxybenzaldehyde (2 equiv) to give, after recrystallization from ethanol, a cream solid (63%): mp 252–253 °C. ¹H NMR (DMSO-*d*₆): 1.52 (4H, br s), 3.22 (4H, q, *J* = 5.8 Hz), 7.23 (4H, m), 7.51 (2H, m), 7.86 (2H, m), 8.47 (2H, s), 8.89 (2H, s), 10.46 (2H, br m). ¹³C NMR (DMSO-*d*₆): 26.1, 39.3, 115.4, 119.5, 121.3, 123.2, 129.3, 133.1, 141.7, 154.0, 155.4, 164.3. HRMS: calculated for C₂₄H₂₂N₄O₄ 431.1719. Found (ESI⁺) (M + H): 431.1707.

***N,N'*-(Butane-1,3-diyl)bis(8-hydroxy-2-imino-2*H*-chromene-3-carboxamide) (25).** Iminodyn-25 was prepared in a similar manner to the synthesis of **14**, from *N,N'*-(butane-1,2-diyl)-bis(2-cyanoacetamide) (**13c**) and 2,3-dihydroxybenzaldehyde (2 equiv) to give, after recrystallization from ethanol, a light-yellow solid (80%): mp 254–256 °C. ¹H NMR (DMSO-*d*₆): 1.55 (4H, br m), 3.46 (4H, q, *J* = 5.8 Hz), 7.14 (4H, s), 7.29 (2H, br m), 8.43 (2H, br m), 8.85 (2H, br m), 10.55 (2H, br s). ¹³C NMR (DMSO-*d*₆): 27.2, 38.4, 119.1, 119.5, 119.9, 126.3, 141.5, 142.1, 143.2, 146.1, 152.1, 162.3. HRMS: calculated for C₂₄H₂₂N₄O₆ 463.1618. Found (ESI⁺) (M + H) 463.1609.

***N,N'*-(Butane-1,3-diyl)bis(7-hydroxy-2-imino-2*H*-chromene-3-carboxamide) (26).** Iminodyn-26 was prepared in a similar manner to the synthesis of **5**, from *N,N'*-(butane-1,2-diyl)-bis(2-cyanoacetamide) (**13c**) and 2,4-dihydroxybenzaldehyde (2 equiv) to give, after recrystallization from ethanol, a yellow solid (88%): mp 276–278 °C. ¹H NMR (DMSO-*d*₆): 1.5 (4H, br m), 3.49 (4H, br), 7.00–7.18 (6H, m), 7.61 (1H, br), 8.26 (2H, s), 9.35 (2H, br), 10.28 (2H, br). ¹³C NMR (DMSO-*d*₆): 28.4, 38.3,

118.1, 119.8, 120.0, 123.2, 141.2, 143.7, 144.2, 149.1, 157.1, 163.8. HRMS: calculated for C₂₄H₂₂N₄O₆ 463.1618. Found (ESI⁺) (M + H) 463.1615.

***N,N'*-(Butane-1,3-diyl)bis(7,8-dihydroxy-2-imino-2*H*-chromene-3-carboxamide) (27).** Iminodyn-27 was prepared in a similar manner to the synthesis of **14**, from *N,N'*-(butane-1,2-diyl)-bis(2-cyanoacetamide) (**13c**) and 2,3,4-trihydroxybenzaldehyde (2 equiv) to give, after recrystallization from ethanol, a dark-red solid (70%): mp > 300 °C. ¹H NMR (DMSO-*d*₆): 1.56 (4H, br), 3.50 (4H, br), 6.73 (2H, d, *J* = 8.4 Hz), 7.13 (2H, d, *J* = 8.5 Hz), 7.69 (2H, br s), 8.30 (2H, s), 9.32 (2H, br s). ¹³C NMR (DMSO-*d*₆): 27.2, 38.0, 118.3, 119.9, 121.8, 125.9, 140.0, 142.1, 149.5, 151.2, 158.1, 164.9. C₂₄H₂₂N₄O₈ calculated: C, 58.30; H, 4.48; N, 11.33. Found: C, 58.87; H, 4.68; N, 12.03

***N,N'*-(Butane-1,3-diyl)bis(6,7-dihydroxy-2-imino-2*H*-chromene-3-carboxamide) (28).** Iminodyn-28 was prepared in a similar manner to the synthesis of **5**, from *N,N'*-(butane-1,2-diyl)-bis(2-cyanoacetamide) (**13c**) and 2,4,5-trihydroxybenzaldehyde (2 equiv) to give, after recrystallization from ethanol, a dark-green solid (64%): mp > 300 °C. ¹H NMR (DMSO-*d*₆): 1.59 (4H, br m), 3.44 (4H, br s), 7.08 (2H, s), 7.19 (2H, s), 7.81 (2H, br s), 9.00 (2H, s), 9.23 (2H, br m). ¹³C NMR (DMSO-*d*₆): 28.6, 39.9, 117.4, 119.4, 120.3, 125.3, 141.1, 146.3, 154.1, 157.3, 165.3. C₂₄H₂₂N₄O₈ calculated: C, 58.30; H, 4.48; N, 11.33; O, 25.89. Found: C, 57.44; H, 5.12; N, 10.87; correct for C₂₂H₂₂N₄O₈ · 0.5H₂O.

***N,N'*-(Pentane-1,3-diyl)bis(2-imino-2*H*-chromene-3-carboxamide) (29).** Iminodyn-29 was prepared in a similar manner to the synthesis of **14**, from *N,N'*-(pentane-1,2-diyl)-bis(2-cyanoacetamide) (**13d**) and 2-hydroxybenzaldehyde (2 equiv) to give, after recrystallization from ethanol, an off white solid (55%): mp 243–245 °C. ¹H NMR (DMSO-*d*₆): 1.32 (2H, quin, *J* = 6.7 Hz), 1.50 (4H, q, *J* = 7.8 Hz), 3.21 (4H, q, *J* = 6.8 Hz), 7.02 (4H, s), 7.15 (2H, br s), 8.43 (2H, br s), 8.86 (2H, br m), 10.49 (2H, br m). ¹³C NMR (DMSO-*d*₆): 22.9, 28.7, 39.2, 18.1, 119.4, 19.9, 123.1, 141.3, 141.9, 142.3, 145.7, 155.3, 162.1. HRMS: calculated for C₂₅H₂₄N₄O₄ 445.1876; (ESI⁺) (M + H) 445.1873

***N,N'*-(Pentane-1,3-diyl)bis(8-hydroxy-2-imino-2*H*-chromene-3-carboxamide) (30).** Iminodyn-30 was prepared in a similar manner to the synthesis of **14**, from *N,N'*-(pentane-1,2-diyl)-bis(2-cyanoacetamide) (**13d**) and 2,3-dihydroxybenzaldehyde (2 equiv) to give, after recrystallization from ethanol, a light-yellow solid (48%): mp 265–267 °C. ¹H NMR (DMSO-*d*₆): 1.28 (2H, quin, *J* = 6.6 Hz), 1.55 (4H, q, *J* = 7.5 Hz), 3.24 (4H, q, *J* = 6.5 Hz), 7.30 (4H, m), 7.50 (2H, m), 7.80 (2H, m), 8.40 (2H, s), 8.91 (2H, br m), 10.52 (2H, br m). ¹³C NMR (DMSO-*d*₆): 24.3, 29.5, 39.3, 14.2, 120.9, 121.9, 125.3, 130.3, 133.1, 141.4, 152.8, 154.3, 164.2. HRMS: calculated for C₂₅H₂₄N₄O₆ 476.1774. Found (ESI⁺) (M + H) 476.1771.

***N,N'*-(Pentane-1,3-diyl)bis(7-hydroxy-2-imino-2*H*-chromene-3-carboxamide) (31).** Iminodyn-31 was prepared in a similar manner to the synthesis of **14**, from *N,N'*-(pentane-1,2-diyl)-bis(2-cyanoacetamide) (**13d**) and 2,4-dihydroxybenzaldehyde (2 equiv) to give, after recrystallization from ethanol, a yellow solid (61%): mp 278–280 °C. ¹H NMR (DMSO-*d*₆): 1.30 (2H, quin, *J* = 6.6 Hz), 1.61 (4H, q, *J* = 7.9 Hz), 3.25 (4H, q, *J* = 6.6 Hz), 7.00–7.18 (6H, m), 7.77 (1H, br s), 8.32 (2H, s), 9.42 (2H, br m), 10.30 (2H, br m). ¹³C NMR (DMSO-*d*₆): 24.1, 29.5, 42.1, 119.0, 122.1, 124.2, 129.3, 141.2, 141.3, 146.4, 150.3, 159.2, 165.3. HRMS: calculated for C₂₅H₂₄N₄O₆ 477.1774. Found (ESI⁺) (M + H) 476.1773

***N,N'*-(Pentane-1,3-diyl)bis(7,8-dihydroxy-2-imino-2*H*-chromene-3-carboxamide) (32).** Iminodyn-32 was prepared in a similar manner to the synthesis of **14**, from *N,N'*-(pentane-1,2-diyl)-bis(2-cyanoacetamide) (**13d**) and 2,3,4-trihydroxybenzaldehyde (2 equiv) to give, after recrystallization from ethanol, a red solid (84%): mp > 300 °C. ¹H NMR (DMSO-*d*₆): 1.30 (2H, quin, *J* = 6.6 Hz), 1.62 (4H, q, *J* = 7.9 Hz), 3.24 (4H, q, *J* = 6.6 Hz), 6.64 (2H, d, *J* = 8.4 Hz), 7.02 (2H, d, *J* = 8.5 Hz), 7.75 (2H, br s), 8.24 (2H, s), 9.35 (2H, br s). ¹³C NMR (DMSO-*d*₆): 24.1,

28.5, 38.7, 118.3, 120.3, 126.2, 129.4, 140.1, 149.4, 150.4, 158.2, 165.3. HRMS: calculated for $C_{25}H_{24}N_4O_8$ 509.1672. Found (ESI⁺) (M + H) 509.1669

***N,N'*-(Pentane-1,3-diyl)bis(6,7-dihydroxy-2-imino-2H-chromene-3-carboxamide) (33)**. Iminodyn-33 was prepared in a similar manner to the synthesis of **14**, from *N,N'*-(pentane-1,2-diyl)bis(2-cyanoacetamide) (**13d**) and 2,4,5-trihydroxybenzaldehyde (2 equiv) to give, after recrystallization from ethanol, a dark-green solid (68%): mp > 300 °C. ¹H NMR (DMSO-*d*₆): 1.30 (2H, quin, *J* = 6.6 Hz), 1.64 (4H, q, *J* = 7.4 Hz), 3.24 (4H, d, *J* = 6.6 Hz), 7.15 (2H, s), 7.23 (2H, s), 7.84 (2H, br m), 9.03 (2H, s), 9.24 (2H, br s). ¹³C NMR (DMSO-*d*₆): 24.1, 28.5, 40.1, 119.2, 120.1, 120.9, 126.2, 139.8, 140.2, 145.3, 152.2, 152.3, 164.2. HRMS: calculated for $C_{25}H_{24}N_4O_8$ 509.1672. Found (ESI⁺) (M + H) 509.1666.

***N,N'*-(Hexane-1,3-diyl)bis(2-imino-2H-chromene-3-carboxamide) (34)**. Iminodyn-34 was prepared in a similar manner to the synthesis of **5**, from *N,N'*-(hexane-1,2-diyl)bis(2-cyanoacetamide) (**13d**) and 2-hydroxybenzaldehyde (2 equiv) to give, after recrystallization from ethanol, an off-white solid (77%): mp 242–244 °C. ¹H NMR (DMSO-*d*₆): 1.32 (4H, m), 1.49 (4H, m), 3.23 (4H, m), 7.14 (4H, m), 7.49 (2H, m), 7.71 (2H, m), 8.36 (2H, s), 8.89 (2H, s), 10.26 (2H, br). ¹³C NMR (DMSO-*d*₆): 26.0, 28.8, 39.5, 114.7, 118.4, 120.3, 123.9, 129.7, 132.6, 140.4, 153.3, 155.4, 161.1. $C_{26}H_{26}N_4O_4$ calculated: C, 68.11; H, 5.72; N, 12.22. Found: C, 68.34; H, 5.89; N, 12.72.

***N,N'*-(Hexane-1,3-diyl)bis(8-hydroxy-2-imino-2H-chromene-3-carboxamide) (35)**. Iminodyn-35 was prepared in a similar manner to the synthesis of **14**, from *N,N'*-(hexane-1,2-diyl)bis(2-cyanoacetamide) (**13e**) and 2,3-dihydroxybenzaldehyde (2 equiv) to give, after recrystallization from ethanol, a light-yellow solid (75%): mp 263–264 °C. ¹H NMR (DMSO-*d*₆): 1.30 (4H, m), 1.53 (4H, m), 3.27 (4H, m), 7.14 (2H, br m), 7.25 (2H, br m), 8.44 (2H, br m), 8.76 (2H, br m), 10.45 (2H, br s). ¹³C NMR (DMSO-*d*₆): 26.4, 29.8, 39.4, 119.0, 119.5, 120.4, 123.8, 141.4, 141.8, 142.8, 146.3, 156.5, 163.2. HRMS: calculated for $C_{26}H_{26}N_4O_6$ 491.1931. Found (ESI⁺) (M + H) 491.1930.

***N,N'*-(Hexane-1,3-diyl)bis(7-hydroxy-2-imino-2H-chromene-3-carboxamide) (36)**. Iminodyn-36 was prepared in a similar manner to the synthesis of **14**, from *N,N'*-(hexane-1,2-diyl)bis(2-cyanoacetamide) (**13e**) and 2,4-dihydroxy-2-hydroxybenzaldehyde (2 equiv) to give, after recrystallization from ethanol, a yellow solid (54%): mp 258–260 °C. ¹H NMR (DMSO-*d*₆): 1.30 (4H, m), 1.51 (4H, m), 3.28 (4H, m), 7.00–7.18 (6H, m), 7.62 (1H, br m), 8.22 (2H, s), 9.32 (2H, br m), 10.23 (2H, br s). ¹³C NMR (DMSO-*d*₆): 26.0, 29.8, 38.4, 118.2, 119.6, 120.0, 124.1, 139.2, 142.1, 144.3, 145.4, 159.3, 165.3. HRMS: calculated for $C_{26}H_{26}N_4O_6$ 491.1931. Found (ESI⁺) (M + H) 491.1921

***N,N'*-(Hexane-1,3-diyl)bis(7,8-dihydroxy-2-imino-2H-chromene-3-carboxamide) (37)**. Iminodyn-37 was prepared in a similar manner to the synthesis of **14**, from *N,N'*-(hexane-1,2-diyl)bis(2-cyanoacetamide) (**13e**) and 2,3,4-trihydroxybenzaldehyde (2 equiv) to give, after recrystallization from ethanol, a red solid (52%): mp > 300 °C. ¹H NMR (DMSO-*d*₆): 1.31 (4H, m), 1.53 (4H, m), 3.30 (4H, m), 6.72 (2H, d, *J* = 8.4 Hz), 7.73 (2H, br m), 8.28 (2H, s), 9.40 (2H, br m). ¹³C NMR (DMSO-*d*₆): 26.1, 29.3, 39.4, 117.3, 119.3, 121.0, 126.2, 140.5, 141.6, 149.4, 151.1, 158.3, 166.5. $C_{26}H_{26}N_4O_8$ calculated: C, 59.77; H, 5.02; N, 10.72. Found: C, 60.11; H, 5.37; N, 11.12.

***N,N'*-(Hexane-1,3-diyl)bis(6,7-dihydroxy-2-imino-2H-chromene-3-carboxamide) (38)**. Iminodyn-38 was prepared in a similar manner to the synthesis of **14**, from *N,N'*-(hexane-1,2-diyl)bis(2-cyanoacetamide) (**13e**) and 2,4,5-trihydroxybenzaldehyde (2 equiv) to give, after recrystallization from ethanol, a dark-green solid (76%): mp > 300 °C. ¹H NMR (DMSO-*d*₆): 1.29 (4H, m), 1.50 (4H, m), 3.28 (4H, m), 7.13 (2H, s), 7.22 (2H, s), 7.85 (2H, br s), 9.01 (2H, s), 9.25 (2H, br m). ¹³C NMR (DMSO-*d*₆): 26.3, 29.3, 38.2, 118.2, 119.2, 119.9, 124.3, 141.1, 141.2, 146.3, 154.1, 157.2, 163.1. HRMS: calculated for $C_{26}H_{26}N_4O_8$ 523.1829. Found (ESI⁺) (M + H) 523.1820.

Acknowledgment. We are grateful for financial support from the National Health and Medical Research Council (Australia), the Children's Medical Research Institute (CMRI), and the University of Newcastle (UoN). This project was also supported by the Epilepsy Research Foundation through the generous support of Finding a Cure for Epilepsy and Seizures. T.A.H. and L.R.O. gratefully acknowledge scholarship support from UoN and CMRI and from UoN, respectively. We thank Sandra Schmid and Sylvia Neumann of The Scripps Research Institute for providing the dynamin II DNA in the pIEx-6 vector plasmid.

References

- (1) McLure, S. J.; Robinson, P. J. Dynamin, endocytosis and intracellular signaling. *Mol. Membr. Biol.* **1996**, *13*, 189–215.
- (2) Cousin, M. A. R.; Robinson, P. J. Mechanisms of synaptic vesicle recycling illuminated by fluorescent dyes. *J. Neurochem.* **1999**, *73*, 2227–2239.
- (3) Cousin, M. A. R.; Robinson, P. J. The dephosphins: dephosphorylation by calcineurin triggers synaptic vesicle endocytosis. *Trends Neurosci.* **2001**, *24*, 659–665.
- (4) Brodin, L. L. P.; Shupliakov, O. Sequential steps in clathrin-mediated synaptic vesicle endocytosis. *Curr. Opin. Neurobiol.* **2000**, *10*, 312–320.
- (5) Hinshaw, J. E. Dynamin and its role in membrane fission. *Annu. Rev. Cell Dev. Biol.* **2000**, *16*, 483–519.
- (6) Zhang, P.; Hinshaw, J. E. Three-dimensional reconstruction of dynamin in the constricted state. *Nat. Cell Biol.* **2001**, *3*, 922–926.
- (7) Sung, J. Y.; Kim, J.; Paik, S. R.; Park, J. H.; Ahn, Y. S.; Chung, K. C. Induction of neuronal cell death by Rab5A-dependent endocytosis of alpha-synuclein. *J. Biol. Chem.* **2001**, *276*, 27441–27448.
- (8) Marks, B.; Stowell, M. H.; Vallis, Y.; Mills, I. G.; Gibbons, A.; Hopkins, C. R.; McMahon, H. T. GTPase activity of dynamin and resulting conformation change are essential for endocytosis. *Nature* **2001**, *410*, 231–235.
- (9) Sever, S. M.; Muhlberg, A. B.; Schmid, S. L. Impairment of dynamin's GAP domain stimulates receptor-mediated endocytosis. *Nature* **1999**, *398*, 481–486.
- (10) McNiven, M. A. Dynamin in disease. *Nat. Genet.* **2005**, *37*, 215–216.
- (11) Zuchner, S.; Noureddine, M.; Kennerson, M.; Verhoeven, K.; Claeys, K.; de Jonghe, P.; Merory, J.; Oliveira, S. A.; Speer, M. C.; Stenger, J. E.; Walizada, G.; Zhu, D.; Pericak-Vance, M. A.; Nicholson, G.; Timmerman, V.; Vance, J. M. Mutations in the pleckstrin homology domain of dynamin 2 cause dominant intermediate Charcot-Marie-Tooth disease. *Nat. Genet.* **2005**, *37*, 289–294.
- (12) Bitoun, M.; Maugren, S.; Jeannot, P. -Y.; Lacène, E.; Ferrer, X.; Laforêt, P.; Martin, J.-J.; Laporte, J.; Lochmüller, H.; Beggs, A. H.; Fardeau, M.; Eymard, B.; Romero, N. B.; Guicheney, P. Mutations in dynamin 2 cause dominant centronuclear myopathy. *Nat. Genet.* **2005**, *37*, 1207–1209.
- (13) Cataldo, A.; Rebeck, G. W.; Ghetti, B.; Hulette, C.; Lippa, C.; Van Broeckhoven, C.; van Duijn, C.; Cras, P.; Bogdanovic, N.; Bird, T.; Peterhoff, C.; Nixon, R. Endocytic disturbances distinguish among subtypes of Alzheimer's disease and related disorders. *Ann. Neurol.* **2001**, *50*, 661–665.
- (14) Metzler, M.; Legendre-Guillemin, V.; Gan, L.; Chopra, V.; Kwok, A.; McPherson, P. S.; Hayden, M. R. HIP1 functions in clathrin-mediated endocytosis through binding to clathrin and adaptor protein 2. *J. Biol. Chem.* **2001**, *276*, 39271–39276.
- (15) Ong, W. Y.; Kumar, U.; Switzer, R. C.; Sidhu, A.; Suresh, G.; Hu, C. Y.; Patel, S. C. Neurodegeneration in Niemann–Pick type C disease mice. *Exp. Brain Res.* **2001**, *141*, 218–231.
- (16) Mukherjee, S.; Ghosh, R. N.; Maxfield, F. R. Endocytosis. *Physiol. Rev.* **1997**, *77*, 759–803.
- (17) Miyauchi, K.; Kim, Y.; Latinovic, O.; Morozov, V.; Melikyan, G. B. HIV enters cells via endocytosis and dynamin-dependent fusion with endosomes. *Cell* **2009**, *137*, 433–444.
- (18) Wang, L.-H.; Rothberg, K. G.; Anderson, R. G. Mis-assembly of clathrin lattices on endosomes reveals a regulatory switch for coated pit formation. *J. Cell Biol.* **1993**, *123*, 1107–1117.
- (19) Gray, J. A.; Sheffler, D. J.; Bhatnagar, A.; Woods, J. A.; Hufeisen, S. J.; Benovic, J. L.; Roth, B. L. Cell-type specific effects of endocytosis inhibitors on 5-hydroxytryptamine 2A receptor desensitization and resensitization reveal an arrestin-, GRK2-, and

- GRK5-independent mode of regulation in human embryonic kidney 293 cells. *Mol. Pharmacol.* **2001**, *60*, 1020–1030.
- (20) Davis, P. J.; Cornwall, M. M.; Johnson, J. D.; Reggianni, A.; Myers, M.; Murtaugh, M. P. Studies on the effects of dansylcadaverine and related compounds on receptor-mediated endocytosis in cultured cells. *Diabetes Care* **1984**, *7* (Suppl. 1), 35–41.
- (21) Larkin, J. M.; Brown, M. S.; Goldstein, J. L.; Anderson, R. G. Depletion of intracellular potassium arrests coated pit formation and receptor-mediated endocytosis in fibroblasts. *Cell* **1983**, *33*, 273–285.
- (22) Lindgren, C. A.; Emery, D. G.; Haydon, P. G. Intracellular acidification reversibly reduces endocytosis at the neuromuscular junction. *J. Neurosci.* **1997**, *17*, 3074.
- (23) Hill, T. A.; Odell, L. R.; Quan, A.; Ferguson, G.; Robinson, P. J.; McCluskey, A. Long chain amines and long chain ammonium salts as novel inhibitors of dynamin GTPase activity. *Bioorg. Med. Chem. Lett.* **2004**, *14*, 3275–3278.
- (24) Quan, A. M.; McGeachie, A. B.; Keating, D. J.; van Dam, E. M.; Rusak, J.; Chau, N.; Malladi, C. S.; Chen, C.; McCluskey, A.; Cousin, M. A.; Robinson, P. J. Myristyl trimethyl ammonium bromide and octadecyl trimethyl ammonium bromide are surface-active small molecule dynamin inhibitors that block endocytosis mediated by dynamin I or dynamin II. *Mol. Pharmacol.* **2007**, *72*, 1425–1439.
- (25) Zhang, J. L.; Lawrance, G. A.; Chau, N.; Robinson, P. J.; McCluskey, A. From Spanish fly to room-temperature ionic liquids (RTILs): synthesis, thermal stability and inhibition of dynamin I GTPase by a novel class of RTILs. *New J. Chem.* **2008**, *32*, 28–36.
- (26) Hill, T. A.; Gordon, C. P.; McGeachie, A. B.; Venn-Brown, B.; Odell, L. R.; Chau, N.; Quan, A.; Mariana, A.; Sakoff, J. A.; Chircop, M.; Robinson, P. J.; McCluskey, A. Inhibition of dynamin I mediated endocytosis by the dynoles—synthesis and functional activity of a family of indoles. *J. Med. Chem.* **2009**, *52*, 3762–3773.
- (27) Hill, T. A.; Odell, L. R.; Edwards, J. K.; Graham, M. E.; McGeachie, A. B.; Rusak, J.; Quan, A.; Abagyan, R.; Scott, J. L.; Robinson, P. J.; McCluskey, A. Small molecule inhibitors of dynamin I GTPase activity: development of dimeric tryphostins. *J. Med. Chem.* **2005**, *48*, 7781–7788.
- (28) Odell, L. R.; Chau, N.; Robinson, P. J.; McCluskey, A. Synthesis and evaluation of dynamin I GTPase photoaffinity labels. *Chem-MedChem* **2009**, *4*, 1182–1188.
- (29) Macia, E.; Ehrlich, M.; Massol, R.; Boucrot, E.; Brunner, C.; Kirchhausen, T. Dynasore, a cell-permeable inhibitor of dynamin. *Dev. Cell* **2006**, *10*, 839–850.
- (30) Otomo, M.; Takahashi, K.; Miyoshi, H.; Osada, K.; Nakashima, H.; Yamaguchi, N. Some selective serotonin reuptake inhibitors inhibit dynamin I guanosine triphosphatase (GTPase). *Biol. Pharm. Bull.* **2008**, *31*, 1489–1495.
- (31) Gazit, A.; Yaish, P.; Gilon, C.; Levitzki, A. Typhostins I: synthesis and biological activity of protein tyrosine kinase inhibitors. *J. Med. Chem.* **1989**, *32*, 2344–2352.
- (32) Burke, T. R.; Lim, B.; Marquez, V. E.; Li, Z. H.; Bolen, J. B.; Stefanova, I.; Horak, I. D. Bicyclic compounds as ring-constrained inhibitors of protein-tyrosine kinase p56lck. *J. Med. Chem.* **1993**, *36*, 425–432.
- (33) McCluskey, A.; Robinson, P. J.; Hill, T.; Scott, J. L.; Edwards, J. K. Green chemistry approaches to the Knoevenagel condensation: comparison of ethanol, water and solvent free (dry grind) approaches. *Tetrahedron Lett.* **2002**, *43*, 3117–3120.
- (34) Correa, W. H.; Edwards, J. K.; McCluskey, A.; McKinnon, I.; Scott, J. L. A thermodynamic investigation of solvent-free reactions. *Green Chem.* **2003**, *5*, 30–33.
- (35) Hill, T. A.; Sakoff, J. A.; Robinson, P. J.; McCluskey, A. Parallel solution-phase synthesis of targeted typhostin libraries with anti-cancer Activity. *Aust. J. Chem.* **2005**, *58*, 94–103.
- (36) Anggono, V.; Cousin, M. A.; Robinson, P. J. Styryl dye-based synaptic vesicle recycling assay in cultured cerebellar granule neurons. *Methods Mol. Biol.* **2008**, *457*, 333–345.
- (37) Ferguson, S. M.; Brasnjo, G.; Hyashi, M.; Wolfel, M.; Collesi, C.; Giovedi, S.; Raimondi, A.; Gong, L. W.; Areil, P.; Paradise, S.; O'Toole, E.; Flavell, R.; Cremona, O.; Miesenbock, G.; Ryan, T. A.; De Camilli, P. A selective activity-dependent requirement for dynamin I in synaptic vesicle endocytosis. *Science* **2007**, *316*, 570–574.
- (38) Robinson, P. J.; Sontag, J.-M.; Liu, J. P.; Fykse, E. M.; Slaughter, C.; McMahon, H. T.; Südhof, T. C. Dynamin GTPase regulated by protein kinase C phosphorylation in nerve terminals. *Nature* **1993**, *365*, 163–166.
- (39) Quan, A.; Robinson, P. J. Rapid purification of native dynamin I and colorimetric GTPase assay. *Methods Enzymol.* **2005**, *404*, 556–569.
- (40) Ogay, I. D.; Lihoradova, O. A.; Azimova, ShS.; Abdugarimov, A. A.; Slack, J. M.; Lynn, D. E. Transfection of insect cell lines using polyethylenimine. *Cytotechnology* **2006**, *51*, 89–98.
- (41) van der Blik, A. M.; Redelmeier, T. E.; Damke, H.; Tisdale, E. J.; Meyerowitz, E. M.; Schmid, S. L. Mutations in human dynamin block an intermediate stage in coated vesicle formation. *J. Cell Biol.* **1993**, *122*, 553–563.
- (42) Sheff, D.; Pelletier, L.; O'Connell, C. B.; Warren, G.; Mellman, I. Transferrin receptor recycling in the absence of perinuclear recycling endosomes. *J. Cell Biol.* **2002**, *156*, 797–804.
- (43) Gaborik, Z.; Hunyady, L. Intracellular trafficking of hormone receptors. *Trends Endocrinol. Metab.* **2004**, *15*, 286–293.
- (44) Dunkley, P. R.; Jarvie, P. E.; Robinson, P. J. A rapid Percoll gradient procedure for preparation of synaptosomes. *Nat. Protoc.* **2008**, *3*, 1718–1728.